



Published in final edited form as:

Curr Mol Med. 2009 May ; 9(4): 435–441.

Novel Imaging Provides New Insights into Mechanisms of Oxygen Transport in Tumors

Matthew E. Hardee¹, Mark W. Dewhirst^{*2}, Nikita Agarwal³, and Brian S. Sorg³

¹ Department of Internal Medicine, Memorial Sloan-Kettering Cancer Center, New York, NY, USA

² Department of Radiation Oncology, Duke University Medical Center, Durham, NC, USA

³ Department of Biomedical Engineering, University of Florida, Gainesville, FL, USA

Abstract

Hypoxia is a common feature of solid tumors, and abnormal tumor oxygen transport is a key factor in the imbalance between tumor oxygen supply and demand. Novel advanced imaging techniques can enable new insights into the complexities of tumor oxygen transport and hypoxia that were not previously known or fully appreciated. In this paper, we document new insights into tumor oxygen transport enabled by spectral imaging of microvascular hemoglobin saturation.

1. INTRODUCTION

Tumor hypoxia has long been known to be an important aspect of tumor physiology and is an independent negative prognostic indicator in solid tumors. As early as 1955, Thomlinson and Gray predicted that the presence of hypoxic cells in tumors would limit the success of radiation treatment. More recently, the presence of intra-tumoral hypoxia has been linked to adverse outcomes regardless of treatment modality as there are multiple mechanisms by which it exerts a negative impact on various treatment types [1–5]. For example, hypoxic tumor cells are more radio-resistant than their more oxygenated counterparts because in radiation-induced cell damage, oxygen reacts with damaged DNA, making it unreparable by cellular machinery [6]. In addition, the cytotoxicity of many commonly used chemotherapeutics is directly affected by hypoxia. This may be due to increased time spent in the G₀ portion of the cell cycle [7], up-regulation of glutathione [8], or by decreased production of nitric oxide [9].

From a molecular medicine viewpoint, there are many opportunities to exploit tumor hypoxia and target hypoxia responsive genes and gene products for therapeutic purposes. The role of HIF-1 in tumor oxygenation and response to therapy, particularly radiation, has been extensively reviewed by our group [10–12]. Erythropoietin (EPO), one of the first identified HIF-regulated gene products, has also been investigated by our group as a potential method of improving tumor oxygenation [13,14], although EPO treatment has been associated with little preclinical improvement in treatment response [15,16] and potentially an increase in tumor growth and angiogenesis [17]. Additionally, adverse outcomes have been reported in several recent clinical trials [18–23], making EPO treatment in cancer patients the subject of recent controversy.

Hypoxia-responsive genes are involved in cell cycle control, apoptosis regulation, angiogenesis, regulation of metabolism and protection of cells from oxidative stress [24]. Up-

*Address correspondence to this author at the Department of Radiation Oncology, Box 3455, Room 201 MSRB, Research Drive, Duke University Medical Center, Durham, NC 27710, USA; Tel: (919) 684-4180; Fax: (919) 684-8718; dewhi001@mc.duke.edu.

regulation of hypoxia-mediated genes may induce p53 mutations and production of pro-angiogenic cytokines leading to increased angiogenesis and metastasis, and a switch to anaerobic metabolism leading to decreased tumor pH [25]. Hypoxia is now regarded as an almost universal feature of solid tumors. Given the significant impact of hypoxia on tumor biology and therapy, it is imperative that the causes and consequences of tumor hypoxia are more widely understood so that rational approaches to the improvement of current therapies and invention of new treatments are possible.

Abnormal oxygen transport is one cause of tumor hypoxia. The traditional view is that diffusion limits of radial oxygen transport from tumor microvessels and acute local stoppages of blood flow are the main mechanisms responsible for hypoxic regions in solid tumors. New imaging technologies enable a more modern perspective that the causes of tumor hypoxia are in many ways more subtle and complex than described by the traditional view alone. In this review, we discuss new insights into tumor hypoxia and oxygen transport gained with spectral imaging of microvascular hemoglobin saturation.

2. TRADITIONAL VIEW OF TUMOR HYPOXIA

Most simply, tissue oxygenation is determined by the balance between oxygen delivery to the tissue and oxygen consumption by the tissue. In normal tissues, this balance is maintained by normally distributed vascular networks, intact vascular signaling pathways, and direct alterations in oxygen consumption [26], all resulting in a “normoxic” environment. However, solid tumors are unable to maintain this balance, resulting in regions of decreased oxygenation and the negative consequences mentioned above.

Classically, two types of hypoxia have been described: chronic, diffusion-limited tumor hypoxia and acute, perfusion-limited hypoxia [27]. However, these two concepts can be viewed as oversimplifications of more complex processes resulting in tumor hypoxia. In reality, there are both spatial and temporal fluctuations in oxygenation. Two types of oxygen gradients within tumors have been identified: (1) radial gradients, resulting from oxygen diffusion limitations, and (2) longitudinal gradients, resulting from depletion of oxygen from hemoglobin as it progressed from the arterial to the venous circulation [28].

One of the factors affecting oxygen gradients within tumors is the irregular vascular network that exists in tumors. Imbalanced expression of various cytokines results in the classic characteristics of tumor vasculature: abnormal branching structures, steep longitudinal gradients along afferent vasculature, decreased numbers of afferent vessels, and uneven distribution of red blood cells at bifurcations. The abnormal vessel architecture results in regions with increased vascular density, where the presence of shunts alters oxygen delivery, and regions with decreased vessel density, where areas of tissue are located beyond the diffusion distance of oxygen. The presence of longitudinal gradients can also contribute to this chronic hypoxia. Axial oxygen gradients are present in arterioles and can be worsened by the absolute decrease in number of afferent vessels within the tumor. The end result is a vessel that is paradoxically hypoxic while still being perfused and resultant hypoxic adjacent tissue.

Tumor oxygen consumption can also contribute to the hypoxic environment, even though tumor cells do not have drastically increased oxygen consumption rates compared to that of normal tissues. However, there is clearly an imbalance between consumption rates and oxygen delivery that will result in hypoxic conditions [29].

It is also clear that oxygenation within the tumor is unsteady and can change in part due to remodeling of tumor vasculature that happens on the scale of days. Transient blood flow has been demonstrated in animal models [30], not only in terms of temporal fluctuations in blood flow, but also heterogeneity in the magnitude and frequency of these fluctuations [31]. Red

cell flux can fluctuate resulting in temporal instability on the order of minutes to hours [32], resulting in fluctuations in perivascular and interstitial pO_2 in tumors. The resulting pO_2 fluctuations can lead to transient hypoxia and repeated hypoxia-reperfusion injury to the adjacent tumor tissue and also the microvascular endothelial cells [33]. Intravascular hypoxia resulting from longitudinal O_2 gradients has also been demonstrated [34]. The overall oxygenation state of the tumor varies with the average magnitude of oxygen delivered and the instability in red cell flux of surrounding microvessels.

3. MODERN VIEWS OF TUMOR HYPOXIA AND OXYGEN TRANSPORT

Microvascular morphological and functional changes are evident from very early stages of cancerous lesion development. Li *et al.* demonstrated increases in host vessel diameter and tortuosity induced by a transformed tumor cell population of about 60–80 cells and the appearance of new functional blood vessels with a tumor mass of about 100 cells [35]. In a rodent model of spontaneous cancer, Hagendoorn *et al.* documented increases in microvascular permeability and tissue interstitial fluid pressure during the hyperplastic/dysplastic stage of lesion development [36]. Spectral imaging measurements of microvessel hemoglobin saturation have shown that tumor-induced increases in host venule diameter and tortuosity are accompanied by increases in venular oxygenation. The increases in venular oxygenation are initially confined to vessels and vessel branches with a more direct connection with the developing tumor, while vessels further away and not directly connected to the tumor are relatively unaffected as shown in Fig. (1).

Sprouting of new blood vessels from existing vessels is one mechanism by which angiogenesis occurs in tumors [37]. Until the sprout makes a functional connection with another vessel, there is no functional blood flow in the sprout and red blood cells can become trapped. Sometimes significant hemorrhaging can occur as erythrocytes leak from an open end in the sprout into the interstitial space. Spectral imaging reveals that in these areas of very active angiogenesis in tumors, a significant area of tissue can contain deoxygenated blood from trapped and hemorrhaged red blood cells before functional blood flow in the neovasculature is established (Fig. 2). Some tumor vascular regions can contain deoxygenated blood despite the proliferation of nearby neovasculature that contains relatively well oxygenated blood (Fig. 3). The sprouts that form in tumors can anastomose with neighboring arterioles. These arteriovenous anastomoses, when part of a tumor microvessel network with chaotic branching and blood flow, can lead to the paradoxical situation in which tumor vascular networks are both supplied and drained by venules [38]. The direct connection between arterioles and venules in tumors may negatively affect treatment by providing a route for blood flow carrying drugs or other therapeutic agent that bypasses a tumor mass [39]. Highly oxygenated blood due to inspired 100% oxygen can also bypass a tumor [40]. An example of this effect is shown in Fig. (4). This phenomenon may explain in part why previous clinical attempts to increase efficacy of radiotherapy by moderating tumor hypoxia with hyperoxic gas breathing at ambient and hyperbaric pressures have had limited success [39,41]. The abnormal response of tumor microvasculature to inspired gases may potentially be exploited, however, for contrast enhanced detection of cancerous lesions [42].

In addition to connections made by arteriovenous anastomoses, direct connections and merging of vessels with highly different hemoglobin saturations can occur in tumor vascular networks during tumor angiogenesis [40]. An example is shown in Fig. (5). The large difference in the oxygenation of the merging vessels can be due to different paths traversed by the vessels through the tumor tissue. For example, if one vessel takes a longer more tortuous path through a greater volume of tumor tissue than the connecting vessel, then it is more likely to have a lower oxygenation at the connection point. Perfusion dynamics within the local network are expected to be influenced by a connection of vessels in this manner because of differences in

the mechanical properties of red blood cells with different oxygenations – less oxygenated red blood cells are stiffer and less deformable than well oxygenated ones [43].

Slow periodic fluctuations in tumor oxygenation have been documented, and recent research suggests that intermittent acute hypoxic episodes from these fluctuations may be more clinically relevant to therapeutic outcome and tumor progression than classically defined chronic and acute hypoxia [40,44–47]. Regional blood flow and oxygen delivery fluctuations also occur in normal tissues and have primarily been attributed to local spontaneous vasomotion. The frequency and character of the fluctuations generally are dependent on the tissue type and animal model. Vasomotion in rabbit cerebral arterioles occurs with a frequency on the order of 0.74cpm (cycles per minute) that is independent of vessel diameter [48]. The frequency of vasomotion in skin skeletal muscle arterioles of Syrian hamsters are generally faster than those in rabbit cerebral arterioles, on the order of 3cpm, and is faster in smaller diameter arterioles [49]. In tumors, dye mismatch experiments to highlight transient blood flow have shown slow temporal fluctuations in blood flow and intratumoral heterogeneity in terms of fluctuation magnitude and frequency [30,31]. Measurements of tumor tissue pO_2 with oxygen microelectrodes revealed slow fluctuations in the range of 0.12 – 0.28cpm [47]. Fluctuations in tumor microvessel oxygenation were observed in the same frequency range with spectral imaging measurements of microvessel hemoglobin saturation [40]. An example of slow fluctuations in a tumor microvessel network is shown in Fig. (6). The oxygenation at a point in tumor tissue is strongly influenced by the surrounding microvasculature, and fluctuations in red cell flux in tumor microvessels can result in transient hypoxia [32,33]. Repeated incidents of transient hypoxia can subject the affected tumor tissue and microvascular endothelial cells to hypoxia-reperfusion injury and thus influence the physiology of the injured cells. Besides affecting the immediately adjacent tumor regions that receive oxygen by diffusion from the microvessels, fluctuations in red cell flux and microvessel oxygenation will affect any downstream tumor areas supplied by the vessels. For some tumor microvessels, the blood oxygenation fluctuations closely follow the fluctuation pattern of nearby normal tissue venules [40].

CONCLUSIONS

While hypoxia is widely recognized as a general feature of solid tumors, the complexities of tumor oxygen transport are still not completely understood or fully appreciated. Novel imaging technologies can enable new insights into tumor oxygen transport to reveal subtle features and effects to increase understanding of this important concept.

Spectral imaging measurements of microvascular hemoglobin saturation have shown that early tumor-induced changes in vascular morphology are accompanied by functional changes as well. This may have important consequences in terms of tumor biology and may also provide a functional signal that can be used for diagnostic and therapeutic monitoring purposes. Spectral imaging also reveals that abnormal tumor angiogenesis can have surprising results, such as connections between microvessels with highly different oxygenations. This phenomenon was not previously observed and it adds another layer of complexity to understanding the mechanics of oxygen transport in tumor microvascular networks. The effect of arteriovenous anastomoses and functionally equivalent structures on tumor oxygen transport with hyperoxic gas breathing was demonstrated with spectral imaging. It is known that venous blood exiting tumors can have increased oxygen content [50], and it is also known that intratumoral shunting of intravenously administered agents can occur [51], but this phenomenon has been underappreciated in terms of clinical attempts to ameliorate tumor hypoxia with hyperoxic gas breathing for therapeutic purposes. Spectral imaging clearly reveals that shunting of oxygenated blood around a tumor can also occur and is a factor that needs to be considered.

In conclusion, spectral imaging has enabled new observations that demonstrate that tumor oxygen transport is an even more dynamic and complex problem than previously appreciated. More research needs to be done to understand the mechanics of tumor oxygen transport completely.

Acknowledgments

The authors acknowledge the contributions of Yiting Cao and Benjamin Moeller (Duke University Medical Center, Durham, NC), and Mamta Wankhede (University of Florida, Gainesville, FL) to original figures presented in this paper. This work was supported in part by a grant from the NIH/NCI CA40355 (MWD).

References

1. Rofstad EK, Sundfor K, Lyng H, Trope CG. *Br J Cancer* 2000;83:354–359. [PubMed: 10917551]
2. Hockel M, Schlenger K, Aral B, Mitze M, Schaffer U, Vaupel P. *Cancer Res* 1996;56:4509–4515. [PubMed: 8813149]
3. Brizel DM, Scully SP, Harrelson JM, Layfield LJ, Bean JM, Prosnitz LR, Dewhirst MW. *Cancer Res* 1996;56:941–943. [PubMed: 8640781]
4. Vaupel P, Schlenger K, Knoop C, Hockel M. *Cancer Res* 1991;51:3316–3322. [PubMed: 2040005]
5. Thomlinson RH, Gray LH. *Br J Cancer* 1995;9:539–549. [PubMed: 13304213]
6. Hall, EJ.; Giaccia, AJ. *Radiobiology for the Radiobiologist*. Lippincott Williams & Wilkins; 2005.
7. Zeman EM, Calkins DP, Cline JM, Thrall DE, Raleigh JA. *Int J Radiat Oncol Biol Phys* 1993;27:891–898. [PubMed: 8244820]
8. Moreno-Merlo F, Nicklee T, Hedley DW. *Br J Cancer* 1999;81:989–993. [PubMed: 10576655]
9. Matthews NE, Adams MA, Maxwell LR, Gofton TE, Graham CH. *J Natl Cancer Inst* 2001;93:1879–1885. [PubMed: 11752013]
10. Moeller BJ, Richardson RA, Dewhirst MW. *Cancer Metastasis Rev* 2007;26:241–248. [PubMed: 17440683]
11. Dewhirst MW, Cao Y, Li CY, Moeller B. *Radiother Oncol* 2007;83:249–255. [PubMed: 17560674]
12. Moeller BJ, Dewhirst MW. *Br J Cancer* 2006;95:1–5. [PubMed: 16735998]
13. Blackwell KL, Kirkpatrick JP, Snyder SA, Broadwater G, Farrell F, Jolliffe L, Brizel DM, Dewhirst MW. *Cancer Res* 2003;63:6162–6165. [PubMed: 14559797]
14. Kirkpatrick JP, Hardee ME, Snyder SA, Peltz CM, Zhao Y, Brizel DM, Dewhirst MW, Blackwell KL. *Radiat Res* 2006;165:192–201. [PubMed: 16518899]
15. Hardee ME, Rabbani ZN, Arcasoy MO, Kirkpatrick JP, Vujaskovic Z, Dewhirst MW, Blackwell KL. *Mol Cancer Ther* 2006;5:356–361. [PubMed: 16505109]
16. Hardee ME, Arcasoy MO, Blackwell KL, Kirkpatrick JP, Dewhirst MW. *Clin Cancer Res* 2006;12:332–339. [PubMed: 16428469]
17. Hardee ME, Cao Y, Fu P, Jiang X, Zhao Y, Rabbani ZN, Vujaskovic Z, Dewhirst MW, Arcasoy MO. *PLoS ONE* 2007;2:e549. [PubMed: 17579721]
18. Henke M, Laszig R, Rube C, Schafer U, Haase KD, Schilcher B, Mose S, Beer KT, Burger U, Dougherty C, Frommhold H. *Lancet* 2003;362:1255–1260. [PubMed: 14575968]
19. Wright JR, Ung YC, Julian JA, Pritchard KI, Whelan TJ, Smith C, Szechtman B, Roa W, Mulroy L, Rudinkas L, Gagnon B, Okawara GS, Levine MN. *J Clin Oncol* 2007;25:1027–1032. [PubMed: 17312332]
20. Smith RE Jr, Aapro MS, Ludwig H, Pinter T, Smakal M, Ciuleanu TE, Chen L, Lillie T, Glaspy JA. *J Clin Oncol* 2008;26:1040–1050. [PubMed: 18227526]
21. Hedenus M, Adriansson M, San Miguel J, Kramer MH, Schipperus MR, Juvonen E, Taylor K, Belch A, Altes A, Martinelli G, Watson D, Matcham J, Rossi G, Littlewood TJ. *Br J Haematol* 2003;122:394–403. [PubMed: 12877666]
22. Thomas G, Ali S, Hoebbers FJ, Darcy KM, Rodgers WH, Patel M, Abulafia O, Lucci JA 3rd, Begg AC. *Gynecol Oncol* 2008;108:317–325. [PubMed: 18037478]

23. Leyland-Jones B, Semiglazov V, Pawlicki M, Pienkowski T, Tjulandin S, Manikhas G, Makhson A, Roth A, Dodwell D, Baselga J, Biakhov M, Valuckas K, Voznyi E, Liu X, Vercammen. *J Clin Oncol* 2005;23:5960–5972. [PubMed: 16087945]
24. Giaccia AJ. *Semin Radiat Oncol* 1996;6:46–58. [PubMed: 10717161]
25. Raghunand N, He X, van Sluis R, Mahoney B, Baggett B, Taylor CW, Paine-Murrieta G, Roe D, Bhujwala ZM, Gillies RJ. *Br J Cancer* 1999;80:1005–1011. [PubMed: 10362108]
26. Pries AR, Reglin B, Secomb TW. *Am J Physiol Heart Circ Physiol* 2001;281:H1015–1025. [PubMed: 11514266]
27. Dewhirst MW. *Adv Exp Med Biol* 2003;510:51–56. [PubMed: 12580404]
28. Cardenas-Navia LI, Richardson RA, Dewhirst MW. *Front Biosci* 2007;12:4061–4078. [PubMed: 17485359]
29. Thews O, Kelleher DK, Hummel M, Vaupel P. *Adv Exp Med Biol* 1999;47:525–532. [PubMed: 10659186]
30. Durand RE, LePard NE. *Acta Oncol* 1995;34:317–323. [PubMed: 7779416]
31. Chaplin DJ, Hill SA. *Br J Cancer* 1995;7:1210–1213. [PubMed: 7779713]
32. Lanzen J, Braun RD, Klitzman B, Brizel D, Secomb TW, Dewhirst MW. *Cancer Res* 2006;66:2219–2223. [PubMed: 16489024]
33. Kimura H, Braun RD, Ong ET, Hsu R, Secomb TW, Papahadjopoulos D, Hong K, Dewhirst MW. *Cancer Res* 1996;56:5522–5528. [PubMed: 8968110]
34. Dewhirst MW, Ong ET, Braun RD, Smith B, Klitzman B, Evans SM, Wilson D. *Br J Cancer* 1999;79:1717–1722. [PubMed: 10206282]
35. Li CY, Shan S, Huang Q, Braun RD, Lanzen J, Hu K, Lin P, Dewhirst MW. *J Natl Cancer Inst* 2000;92:143–147. [PubMed: 10639516]
36. Hagendoorn J, Tong R, Fukumura D, Lin Q, Lobo J, Padera TP, Xu L, Kucherlapati R, Jain RK. *Cancer Res* 2006;66:3360–3364. [PubMed: 16585153]
37. Carmeliet P, Jain RK. *Nature* 2000;407:249–257. [PubMed: 11001068]
38. Vaupel P, Kallinowski F, Okunieff P. *Cancer Res* 1989;49:6449–6465. [PubMed: 2684393]
39. Hockel M, Schlenger K, Hockel S, Aral B, Schaffer U, Vaupel P. *Int J Cancer* 1998;79:365–369. [PubMed: 9699528]
40. Sorg BS, Hardee ME, Agarwal N, Moeller BJ, Dewhirst MW. *J Biomed Opt* 2008;13 article 014026.
41. Siemann, DW.; Horsman, MR.; Chaplin, DJ. Modification of oxygen supply. In: Molls, M.; Vaupel, P., editors. *Blood perfusion and microenvironment of human tumors*. Berlin: Springer-Verlag; 1998. p. 209-217.
42. Kotz KT, Dixit SS, Gibbs AD, Orduna JM, Haroon Z, Amin K, Faris GW. *Opt Express* 2008;16:19–31. [PubMed: 18521129]
43. Kavanagh BD, Coffey BE, Needham D, Hochmuth RM, Dewhirst MW. *Br J Cancer* 1993;67:734–741. [PubMed: 8471430]
44. Dewhirst MW. *Cancer Res* 2007;67:854–855. [PubMed: 17283112]
45. Martinive P, Defresne F, Bouzin C, Saliez J, Lair F, Grégoire V, Michiels C, Dessy C, Feron O. *Cancer Res* 2006;66:11736–11744. [PubMed: 17178869]
46. Rofstad EK, Galappathi K, Mathiesen B, Ruud EBM. *Clin Cancer Res* 2007;13:1971–1978. [PubMed: 17360973]
47. Braun RD, Lanzen JL, Dewhirst MW. *Am J Physiol* 1999;277:H551–H568. [PubMed: 10444480]
48. Hundley WG, Renaldo GJ, Levasseur JE, Kontos HA. *Am J Physiol* 1998;254:H67–71. [PubMed: 3337261]
49. Colantuoni A, Bertuglia S, Intaglietta M. *Int J Microcirc Clin Exp* 1994;14:151–158. [PubMed: 8082994]
50. Warren, BA. The vascular morphology of tumors. In: Peterson, H-I., editor. *Tumor blood circulation: Angiogenesis, vascular morphology and blood flow of experimental and human tumors*. Boca Raton: CRC Press, Inc; 1979. p. 1-47.
51. Mariani L, Schroth G, Wielepp JP, Haldemann A, Seiler RW. *Neurosurgery* 2001;48:353–358. [PubMed: 11220379]

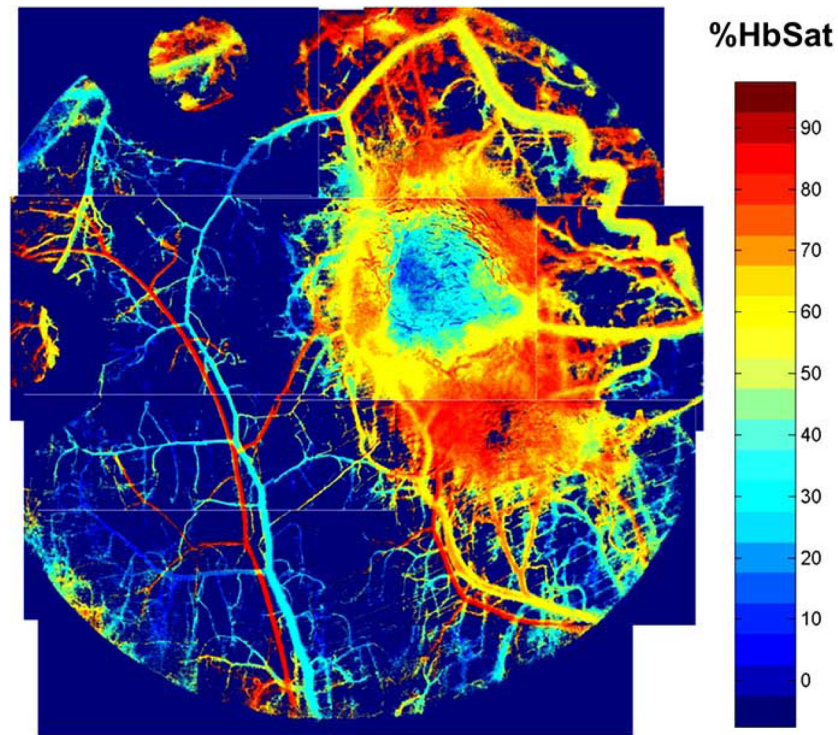


Fig. (1). Photomontage of microvascular hemoglobin saturation in a 4T1 mouse mammary carcinoma grown in a nude mouse dorsal skin window chamber. Pixels are colored according to the hemoglobin saturation values in the scale bar, with background the lowest color on the scale (under the 0% saturation color). Venules with branches directly connected to the tumor are tortuous, dilated, and have increased oxygenation compared to normal appearing venules at a distance from the tumor. The window chamber is 12mm diameter.

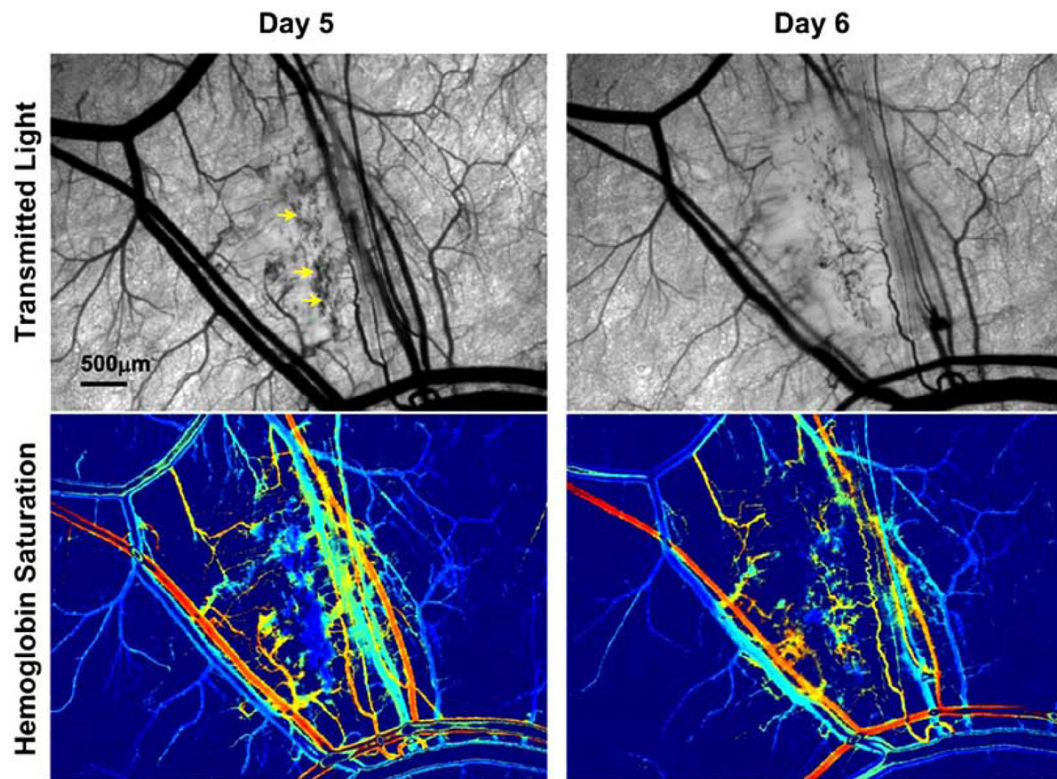


Fig. (2). 4T1 mouse mammary adenocarcinoma five and six days after implantation of tumor cells. A large region of deoxygenated red blood cells (arrows in transmitted light image) is seen on day five due to entrapment in vessel sprouts and hemorrhaging from extensive regional angiogenesis. Patent vessels established in the area on day six help supply oxygenated blood to some areas in the region while others areas remain deoxygenated. The color scale for the hemoglobin saturation image is the same as that in Fig. (1).

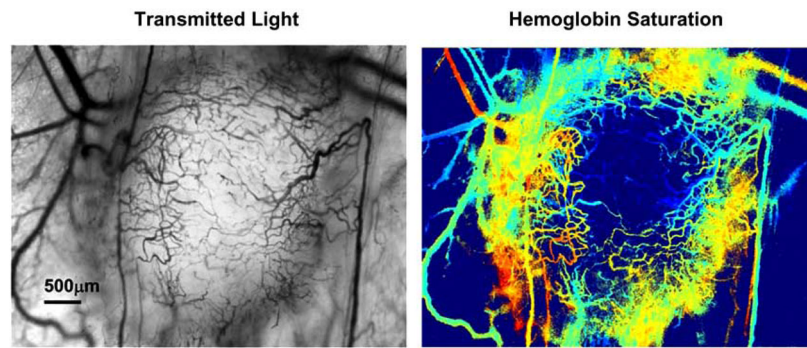


Fig. (3). Tumor with a large region of deoxygenated blood despite proliferation of nearby neovasculature with relatively higher oxygenation. This is the same tumor as in Fig. (4) at a later time point. The color scale for the hemoglobin saturation image is the same as that in Fig. (1).

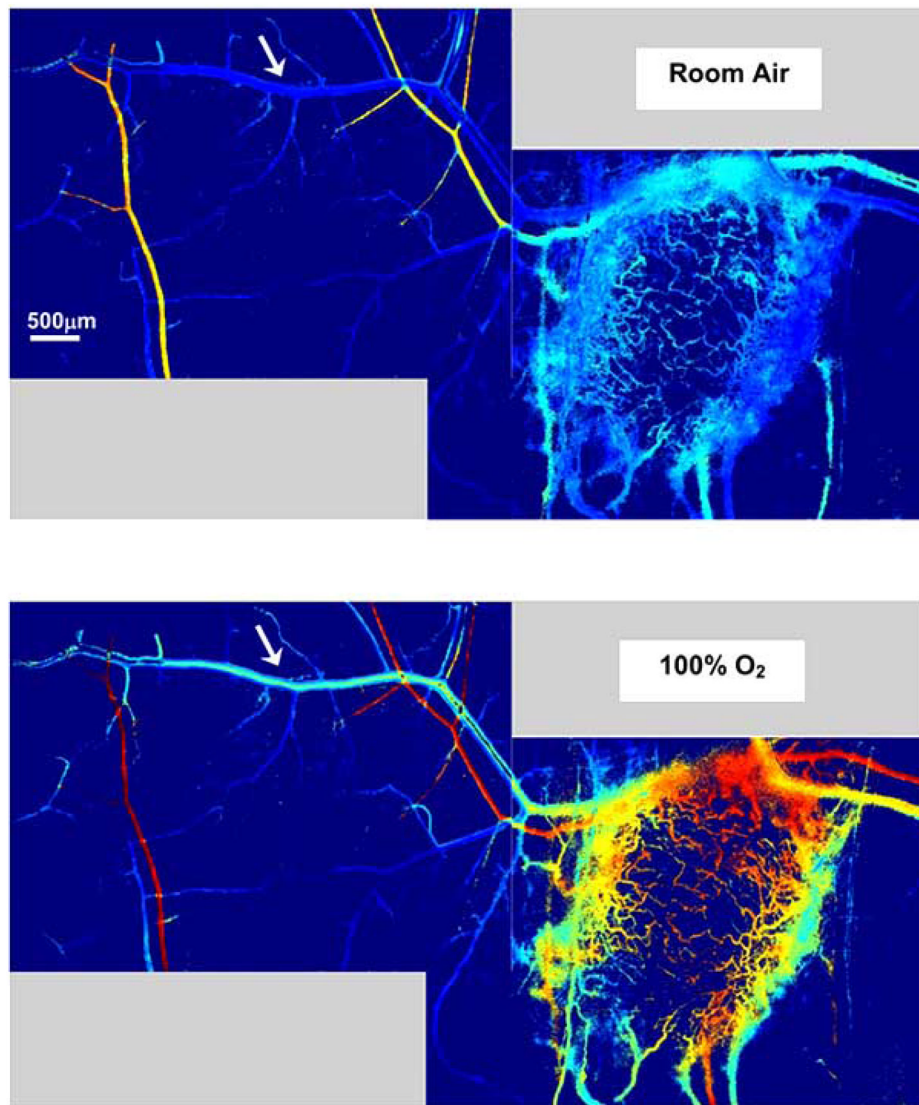


Fig. (4). Oxygenated blood from inspired 100% O₂ can bypass a tumor from arterioles to venules. A host venule (arrow) with branches in intimate contact with a 4T1 tumor has significantly increased oxygenation upon a switch from breathing room air to 100% O₂. Non-tumor associated branches from this venule are relatively unaffected by the switch to oxygen breathing. The color scale for the hemoglobin saturation image is the same as that in Fig. (1).

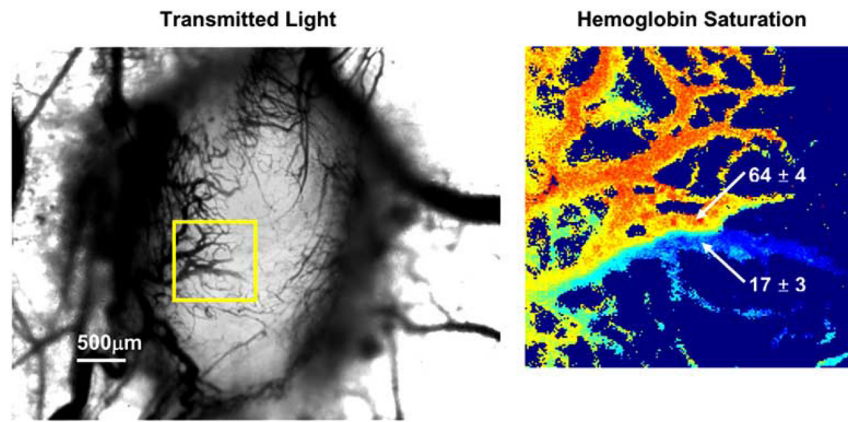


Fig. (5). Example of two merging vessels with highly different oxygenations. The hemoglobin saturation map area is indicated by the boxed region in the transmitted light image. The percent hemoglobin saturation of the indicated vessels is given as the mean \pm standard deviation of a small region of pixels in the image. The color scale for the hemoglobin saturation image is the same as that in Fig. (1).

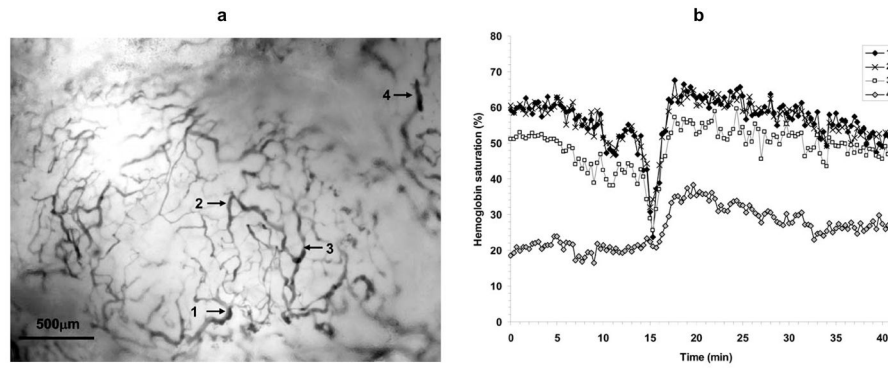


Fig. (6). Oxygenation fluctuations in microvasculature of a 4T1 tumor. **(a)** Transmitted light image of tumor with regions of interest indicated. **(b)** Hemoglobin saturation of the indicated regions. Measurements were acquired every 20s. Slow fluctuations can be seen that generally follow the same temporal pattern although there are microregional differences. A deoxygenation spike occurs around 15min in regions 1–3 that is not present in region 4, and regions 3 and 4 have different average oxygenations compared to regions 1 and 2.